Electronic Supplementary Information

An X-ray transparent microfluidic platform for screening of the phase behavior of lipidic mesophases

D. S. Khvostichenko, E. Kondrashkina, S. L. Perry, A. S. Pawate, K. Brister, P. J. A. Kenis

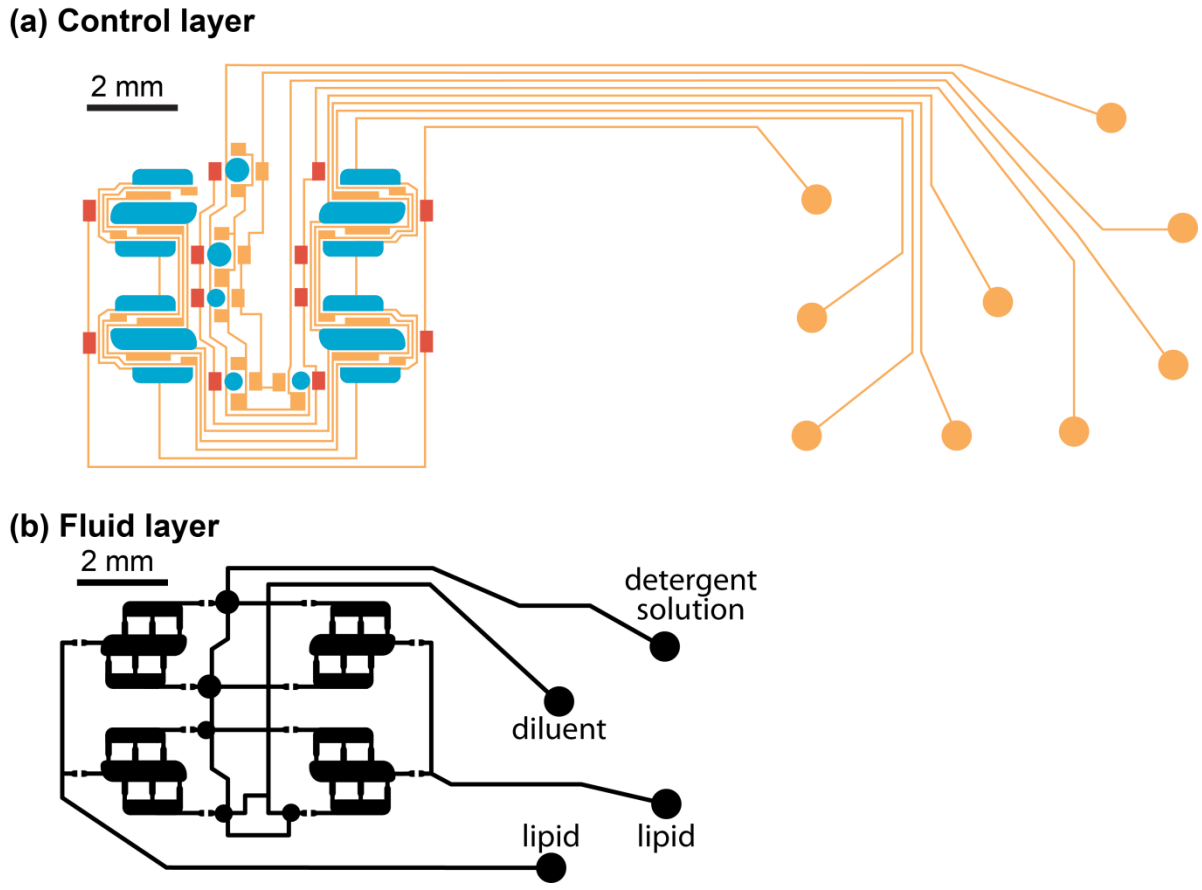

Figure S1. (a) Control and **(b)** fluid layer of the microfluidic platform for screening of lipidic mesophases. Circles at ends of lines designate the locations of inlet ports. Control layer: orange, normally open routing valves; red, normally closed routing valves; blue, injection valves. Designations of inlet ports are indicated for the fluid layer.

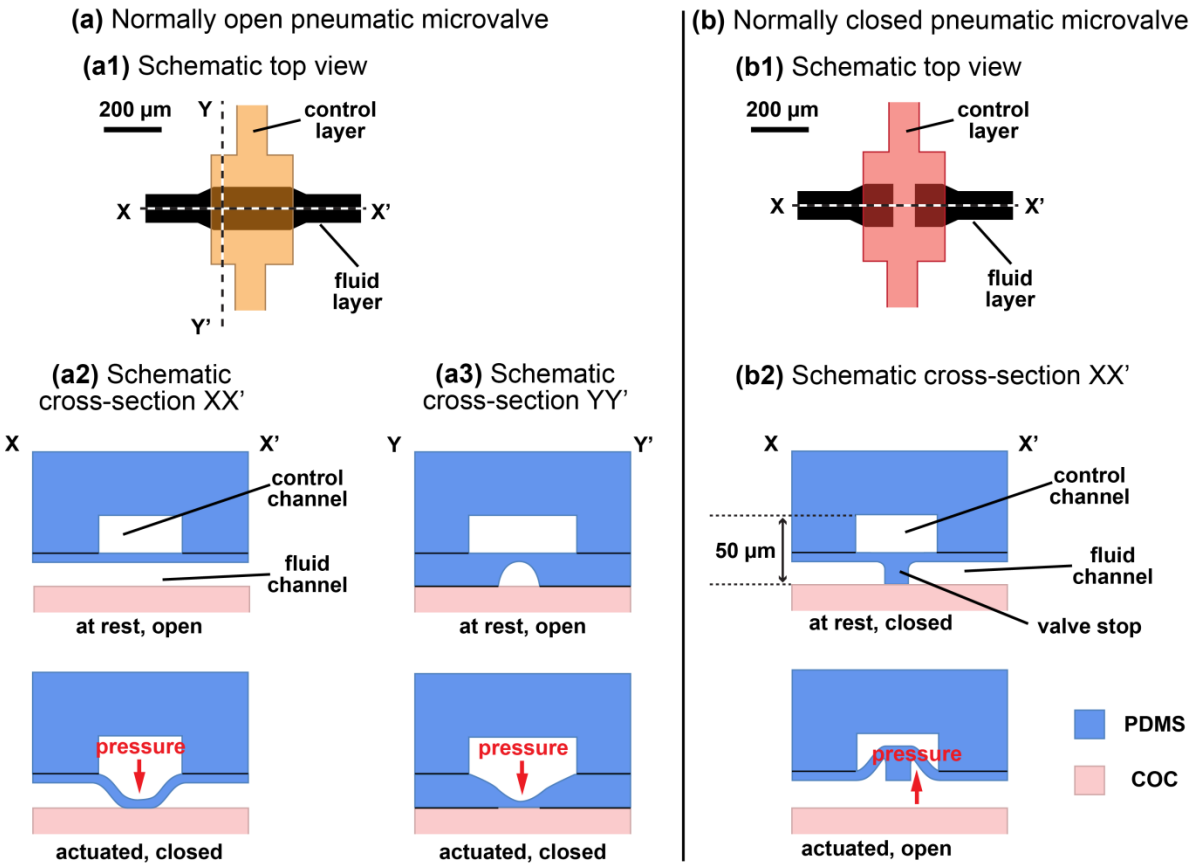

Figure S2. Schematic top view and design and operation of **(a)** normally open and **(b)** normally closed pneumatic elastomeric microvalves fabricated in PDMS. **(a1, b1)** Top view of the control (orange or red) and fluid (black) layer channels. **(a2, b2, b3)** Schematic cross-section of the microvalve. Only the height of the fluid layer and the control channel are drawn to scale. The red arrows indicate direction of the pressure gradient (higher pressure → lower pressure) required for valve actuation. Black lines between layers indicate areas that are irreversibly bonded. **(a)** In a normally open microvalve flow in the fluid channel is restricted by **(a2, a3)** membrane deflection upon positive pressure application to the control channel. **(a3)** A rounded channel profile is required for reliable isolation.[1] **(b)** In a normally closed microvalve,[2] a valve stop fabricated in the fluid layer isolates sample compartments without external actuation. The valve stop reversibly adheres to the substrate due to adhesive properties of PDMS. The valve opens due to the deflection of a thin elastomeric membrane if vacuum is applied to the control channel or if positive pressure is applied to the fluid channel. In our fabrication protocol vacuum was applied to the control channel in the PDMS/substrate bonding step to avoid permanent bonding between the valve stop and the substrate. Positive pressure to the fluid channel was applied during device filling. Additionally, positive pressure was applied to the normally closed microvalves during mixing to keep them closed under conditions of high pressure in the fluid layer that exceeded their actuation pressure.[2]

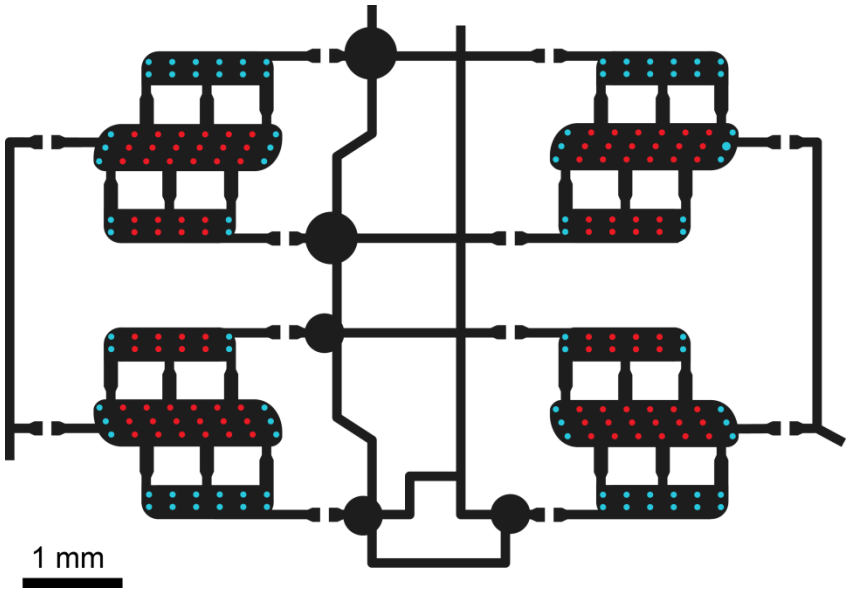

Figure S3. Locations probed in a device during SAXS data collection (red and cyan) are overlaid with the design of the fluid layer (black) of the device. The size of the dots is bigger than the footprint of the X-ray beam for visual clarity. Red points indicate measurements used for the calculation of relative amounts and lattice parameters of mesophase. Cyan points indicate measurements that were excluded as explained below. The end points of each row of datapoints were excluded to avoid artifacts related to cross-talk between sample compartments and fluidic lines. We also noticed systematic differences within a given mixer (sample) between lattice parameters of samples in side chambers closest to the edges of the device and the other two chambers of the mixer. The lattice parameters of samples in the outer chambers were smaller than the lattice parameters of the central mixer chambers and the side mixer chambers facing the center of the device, likely due to adsorption of water into PDMS. Thus, data points corresponding to outer chambers of mixers were also excluded in the averaging of lattice parameters and relative amounts of mesophases for every device tested. We did not observe systematic differences between the lattice parameters of samples in the central chamber of the mixer and the side chamber facing the center of the device in a given mixer.

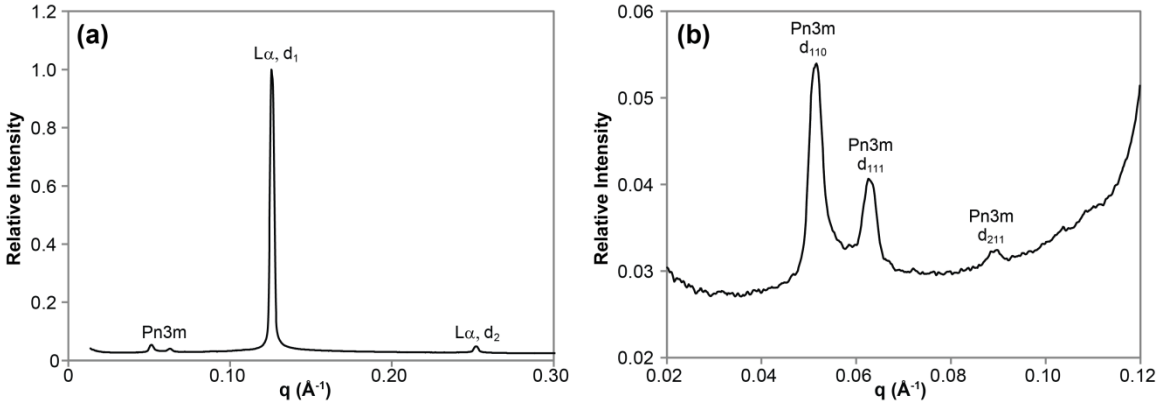

Figure S4. (a) A diffraction pattern of a sample containing *Pn3m* and *Lα* phases in a glass capillary collected after a 2 h equilibration at 25 °C and **(b)** a magnified view of Pn3m reflections. Sample composition: MO/detergent solution ratio 55:45 w/w; detergent solution: 10% βOG in 25 mM NaH_2PO_4, pH 5.5. Lattice parameters of mesophases: *Pn3m*, 174 Å; *Lα*, 50.1 Å.

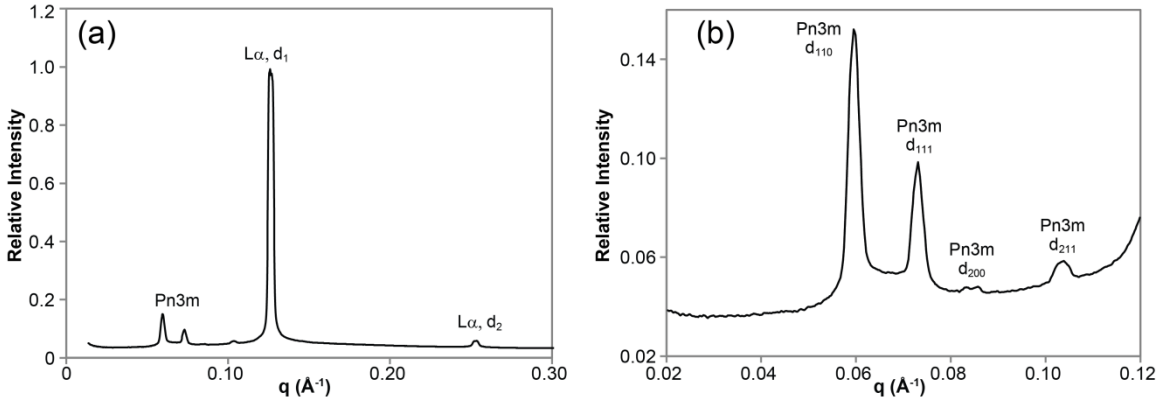

Figure S5. (a) A diffraction pattern of a sample containing *Pn3m* and *Lα* phases in a glass capillary collected after 24 h equilibration at 25 °C and **(b)** magnified view of *Pn3m* reflections. Sample thickness ~0.9 mm. Sample composition: MO/detergent solution ratio 55:45 w/w; detergent solution: 10% βOG in 25 mM NaH_2PO_4, pH 5.5. Lattice parameters of mesophases: *Pn3m*, 150 Å; *Lα*, 50.0 Å.

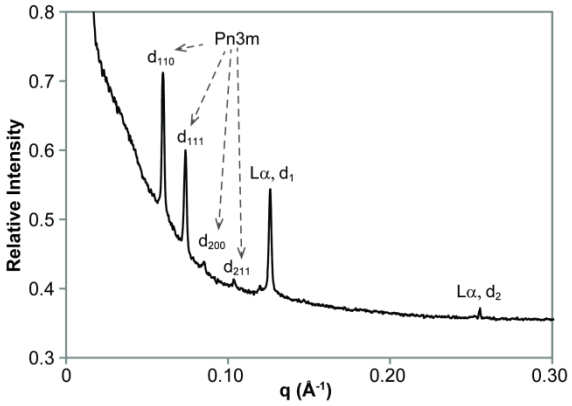

Figure S6. Diffraction pattern of an on-chip sample containing *Pn3m* and *Lα* phases. Sample thickness ~15 μm. Sample composition: MO/detergent solution ratio 55:45 w/w; detergent solution: 10% βOG in 25 mM NaH_2PO_4, pH 5.5. Lattice parameters of mesophases: *Pn3m*, 148 Å; *Lα*, 49.8 Å.

Estimating Relative Amounts of Mesophases

Amounts of mesophases in each sample were estimated based on the intensity of the highest-intensity reflection d_{max} of a given mesophase (d_1 for *Lα*, d_{111} for *Ia3d*, d_{110} for *Pn3m*). Raw diffractograms were integrated in Fit2D (v. 12.077, A.P. Hammersley, ESRF) from scattering angle θ = 0° to θ = 4° in 0.001333° increments for a total of 3000 points for each integrated diffractogram. Integrated diffractograms were processed in Matlab (R2008a, v. 7.6.0.324, The MathWorks Inc., Natick, MA).

The intensity corresponding to a given phase $I_{phase}^{\max}$ was read from the diffractogram based on the value of lattice parameter in the phase assignment:

$$\theta_{\max} = \operatorname{asin}\left(\frac{\lambda}{2a/\sqrt{h_{\max}+k_{\max}+l_{\max}}}\right) \quad (1)$$

$$I_{phase}^{\max} = I^{corr}(\theta_{\max}) \quad (2)$$

where a is the lattice parameter of a given phase, h_{max}, k_{max}, and l_{max} are the *hkl* indices of the highest-intensity reflection of a given phase, λ is the wavelength of the incident X-ray beam, I^{corr} is the intensity of the diffractogram after baseline correction to account for scattering around the beamstop, which is comparable in the intensity to the intensity of the sample (see Figures 4 and S3).

Fluctuations of beam intensity during data collection, typical for synchrotron X-ray sources, could result in variations in signal intensity from otherwise identical samples. To crudely account for the fluctuations, we used the scattering intensity around the beamstop, free from *hkl* reflections, as a measure of beam intensity for each diffractogram:

$$I_{beam} = \frac{\sum_{n(\theta=0.15)}^{n(\theta=0.20)} I(n)}{n(\theta=0.20)-n(\theta=0.15)} - \frac{\sum_{n(\theta=2.5)}^{n(\theta=4.0)} I(n)}{n(\theta=4.0)-n(\theta=2.5)} \quad (3)$$

where $n(\theta)$ is the number of data point in the diffraction angle – diffraction intensity array corresponding to a given value of θ. For the calculations of sample composition the beam intensity-adjusted value of sample intensity was used:

$$I_{phase}^{adj} = \frac{I_{phase}^{\max}}{I_{beam}} \quad (4)$$

A value of "unit" signal intensity I_{phase}^{unit} was calculated for each mesophase type. This value corresponds to a sample containing a given phase type only, i.e., 100% of *Pn3m*, *Ia3d*, or *Lα*. For *Ia3d*

and *Lα* phases available data points containing a single mesophase type were used to estimate the average "unit" signal intensity corresponding to 100% of a given phase type in the sample:

$$I_{phase}^{unit} = \frac{\sum_{j} I_{phase}^{adj}(j)}{j_{phase\_only}} \qquad (5)$$

where *j* spans only diffractograms containing solely a given mesophase type and j_{phase_only} is the number of such diffractograms for a given phase type. Lattice parameters of mesophases were identical in data points with a single mesophase type and with multiple mesophase types, suggesting identical compositions and invariance of intensity/amount relationships. For the *Pn3m* mesophase no such data were available because it was always observed together with at least one other phase. We used the model of Garstecki and Holyst[3,4] for scattering patterns of cubic phases to estimate the unit signal intensity for the *Pn3m* phase. In the model the intensity I_{hkl}^{mod} of a given *hkl* reflection of a mesophase is given by:

$$I_{hkl}^{\mathrm{mod}} = M_{hkl}\left[F_{hkl}^{S*}\frac{\sin\left(\alpha_{hkl}\ \pi\left(h^2+k^2+l^2\right)^{1/2} L/a\right)}{\alpha_{hkl}\ 2\pi\left(h^2+k^2+l^2\right)^{1/2}}\right]^2 \qquad (6)$$

where *L* is the lipid bilayer thickness in the mesophase and parameters F_{hkl}^{S*}, α_{hkl}, and M_{hkl} are constants for a given phase type and *hkl* reflection, given by Garstecki and Holyst.[3] Reflections *110* and *111* for *Pn3m* and *Ia3d* phases, respectively, were used to extract diffraction signal intensity. Hence, the unit signal intensity for the *Pn3m* phase can be estimated as:

$$I_{Pn3m}^{(unit)} = \frac{I_{Ia3d}^{(unit)}}{I_{111,Ia3d}^{(\mathrm{mod})}} \cdot I_{110,Pn3m}^{(\mathrm{mod})} \qquad (7)$$

In the calculations of I_{hkl}^{mod} the value of the bilayer thickness *L = 34.6 Å* was selected based on the correlation for MO/water mesophases by Briggs et al.;[5] the value does not change appreciably when detergent is added.[6] Values of lattice parameters used in the calculation were *a(Pn3m) = 148 Å*, *a(Ia3d) = 180 Å*.

Finally, for each lipidic mixer the average intensity of a given phase in the mixer is:

$$I_{phase}^{mixer} = \frac{\sum_{j} I_{phase}^{adj}(j)}{j_{phase\_mixer}} \qquad (8)$$

where j spans the diffractograms in the mixer that contain a given mesophase type and j_{phase_mixer} is the number of such diffractograms for a given mixer. The average amount of the mesophase v_{phase}^{mixer} in the mixer is then:

$$v_{phase}^{mixer} = \frac{I_{phase}^{mixer}}{I_{phase}^{unit}} \tag{9}$$

Ideally, the sum of values of v for different phases in the mixer must add up to unity. However, this was not the case here because certain parameters, such as the thickness of the sample and the beam intensity could not be controlled precisely during data collection. Thus, the data were additionally rescaled:

$$\phi_{phase}^{mixer} = \frac{v_{phase}^{mixer}}{v_{Pn3m}^{mixer} + v_{Ia3d}^{mixer} + v_{L\alpha}^{mixer}} \cdot 100\% \tag{10}$$

If a certain phase type was absent in the mixer, the corresponding value of v was set to zero. Values of θ are reported in Figure 5. Based on the non-uniformity of signal intensities for $L\alpha$ phases we estimate the relative error of ±20% in the calculations of θ.

References:

1 M. A. Unger, H.-P. Chou, T. Thorsen, A. Scherer and S. R. Quake, *Science*, 2000, **288**, 113-116.
2 R. Mohan, B. R. Schudel, A. V. Desai, J. D. Yearsley, C. A. Apblett and P. J. A. Kenis, *Sensors Actuators B*, 2011, **160**, 1216-1223.
3 P. Garstecki and R. Hołyst, *Langmuir*, 2002, **18**, 2519-2528.
4 P. Garstecki and R. Hołyst, *Langmuir*, 2002, **18**, 2529-2537.
5 J. Briggs, H. Chung and M. Caffrey, *J. Phys. II*, 1996, 723-751.
6 B. Angelov, A. Angelova, M. Ollivon, C. Bourgaux and A. Campitelli, *J. Am. Chem. Soc.*, 2003, **125**, 7188-7189.